Appl. Magn. Reson. 10, 55–69 (1996)

Applied Magnetic Resonance

Two Dimensional FT-EPR Spectroscopy for Spin-Correlated Radical Pairs – Application to Photoinduced Electron Transfer Reaction between ZnTPPS and DQ in a Micellar Solution

R. Hanaishi, K. Yamamoto, Y. Ohba, S. Yamauchi, and M. Iwaizumi

Institute for Chemical Reaction Science, Tohoku University, Sendai, Japan

Received June 19, 1995

Abstract. Two pulsed EPR methods for studying spin-correlated radical pairs (SCRPs) transiently generated in photochemical reactions are presented. One is two dimensional (2D) EPR nutation method which uses anomalous flip angle dependence of SCRPs for microwave (MW) pulses and the other is application of the so called 2D J spectroscopy in NMR to studies of paramagnetic SCRPs. The methods were applied to observation of the SCRP generated in the photoinduced electron transfer reaction between zinctetraphenylporphyrinsulphonate (ZnTPPS) and duroquinone (DQ) in cetyltrimethylammonium chloride (CTAC) micellar solution in which SCRP alives for a relatively long period at the early stage of the reaction processes.

1. Introduction

Time resolved EPR spectroscopy has been widely and effectively used for investigations of spin and reaction dynamics in photochemical reactions involving radical intermediates [1, 2]. In EPR studies of these photochemical reactions, spin correlated radical pairs (SCRPs) are sometimes observed, but their signals are usually overlapped with those of dissociated radicals. Attempts to study such SCRPs have been made in a wide field activity [3–6]. Recently developed FT-EPR spectroscopy yields more detailed information about kinetics and structures of SCRPs and other transient radicals, with aids of its excellent time and frequency resolution and its high sensitivity [2]. However, most remarkable features of the pulsed EPR spectroscopy is availability of multi-dimensional methods which are useful to extract some specific information from total spectra as have been shown in NMR spectroscopy [7]. The SCRPs seem to be one of the most interesting challenging subjects for the 2D EPR spectroscopy.

In this paper, we present two attempts for observation of SCRPs. One is 2D EPR nutation spectroscopy, which uses anomalous flip angle dependence of SCRPs for microwave (MW) pulses and the other is application of the so called

2D J spectroscopy in NMR [7] to examination of spin-spin couplings in SCRPs. The spin-spin interaction in SCRPs is analogous to a scalar spin-spin coupling between nuclear spins in NMR in liquid. However, SCRPs are created in a thermally non-equilibrium spin state. Harashanori *et al.* [8] and Kroll *et al.* [9] have shown an anomalous flip angle dependence of SCRPs. The SCRPs have nutation frequencies corresponding to twice of those of dissociated radicals. Similar situation was pointed out in CIDNP of FT-NMR by Ernst and his coworkers [10]. We pay attention to such anomalous flip angle dependence of SCRPs and apply it to the 2D nutation method to observe the SCRPs.

On the other hand, the SCRPs show absorption/emission or emission/absorption antiphase doublet signals. It can be shown that when the spectrum is obtained by Fourier transformation of FID signals on electron-spin-echo (ESE), the antiphase SCRP signals change their phase as a function of $4\pi J t_1$, where t_1 is time separation between the two MW pulses in ESE experiments. We use this feature in ESE-FT-EPR for studies of spin-spin interaction J in SCRPs.

We applied these two methods to the photo-induced electron transfer reaction between zinctetraphenylporphyrin sulfonate (ZnTPPS) and duroquinone (DQ) in cetyltrimethylammonium chloride (CTAC) micellar solution. This system has been well investigated by one dimensional time resolved FT-EPR spectroscopy by Willigen *et al.* [10] and it has been shown that the SCRP formed in the reaction alives for a relatively long period by being trapped in micelles.

2. Methods and Theory

2.1. 2D FT-EPR Nutation Method

2D FT-EPR nutation spectra are measured by the pulse sequence shown in Fig. 1a. After the laser pulse, a MW pulse is applied during t_1 and subsequent quadrature FID is sampled along t_2. The experiments are done in a series of various t_1 giving 2D complex FID $s(t_1, t_2)$ which are Fourier transformed in both dimensions to give the 2D nutation spectrum $s(\Omega_1, \Omega_2)$. Here Ω_1 and Ω_2 are nutation frequencies and ordinary EPR frequencies, respectively. Details of the theory for this 2D FT-EPR nutation method has been presented in our previous paper [12]. So, we present only its summary here.

Although the exchange interaction J will dynamically vary with time by motion of the radicals in SCRP in solvent cage, we approximate it to be kept constant during the data sampling for simplicity. Time evolution of the spin density operator σ in a rotating frame for the MW pulse sequence is expressed by the well known Liouville von Neuman equation [13] as

$$\sigma(t_1, t_2) = \exp(-\mathrm{i}\mathscr{H}_0 t_2)\exp[-\mathrm{i}(\mathscr{H}_0 + \mathscr{H}_\mathrm{p})t_1]\sigma(0) \times \exp[\mathrm{i}(\mathscr{H}_0 + \mathscr{H}_\mathrm{p})t_1]\exp(\mathrm{i}\mathscr{H}_0 t_2) \ . \quad (1)$$

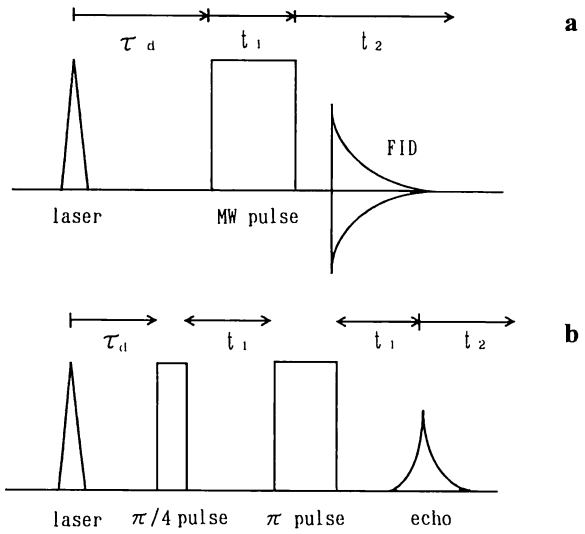

Fig. 1. Pulse sequences for **a** 2D FT-EPR nutation method and **b** ESE J method, respectively.

Here $\mathscr{H}_0$ is the unperturbed Hamiltonian of SCRP, $\mathscr{H}_p$, is the Hamiltonian for the interaction of the spins with the MW pulse, and t_1 and t_2 are evolution times with and without MW pulse, respectively.

Under the high field approximation, the spin Hamiltonian of SCRP in the rotating frame is expressed as

$$\mathscr{H}_0 = \frac{h}{2\pi}(\Omega_a S_{az} + \Omega_b S_{bz}) - hJ\left(2\mathbf{S}_a \cdot \mathbf{S}_b + \frac{1}{2}\right), \tag{2}$$

where hJ is an isotropic exchange interaction energy between two radicals a and b in the SCRP, and Ω_a and Ω_b represent offset frequencies of the radicals a and b in the reference frame, respectively. When the MW field faces to the $-y$ axis, $\mathscr{H}_p$, is written as

$$\mathscr{H}_p = -\gamma_a \frac{h}{2\pi} B_1 S_{ay} - \gamma_b \frac{h}{2\pi} B_1 S_{by} \tag{3}$$

and the FID signals are given by

$$s(t_1, t_2) = \mathrm{Tr}[(S_x + \mathrm{i}\, S_y)\sigma(t_1, t_2)] \ . \tag{4}$$

2D Fourier transformation of $s(t_1, t_2)$ gives 2D nutation spectrum $s(\Omega_1, \Omega_2)$.

Analytical expressions for the nutation frequencies of SCRPs were given in the previous paper [12]. They were derived under the assumption that the exchange

interaction $h|J|$ is much smaller than the interaction between the spins and the MW field, and also $2\pi|J|$ is smaller than the difference between the offset frequencies of the two electron spins $|\Omega_a - \Omega_b|$. The expressions obtained there indicate the followings. 1) Four nutation frequencies appear; they are not only the frequencies corresponding to sum of the two radicals $\Omega_a + \Omega_b$ which are pointed out by Harshanori *et al.* [8] and Kroll *et al.* [9], but also the difference frequency of the two radicals, $\Omega_a - \Omega_b$, as well as the frequencies for the isolated radicals Ω_a and Ω_b. 2) The relative intensity of each component depends on the initial density matrix as well as also to the resonance offset of the partner spin.

In the present case, because of the short T_2^* value of the ZnTPPS radical, the observed FID consists of only contribution of the DQ radical. The magnetization of the SCRP is, hence, obtained by taking trace of the spin density matrix over the subspace of the ZnTPPS radical as the following:

$$\sigma_{DQ}(t_1, t_2) = \mathrm{Tr}_{ZnTPPS}[\sigma(t_1, t_2)]$$

$$= \mathrm{Tr}_{ZnTPPS}\left[\begin{array}{c} \begin{matrix} \alpha\alpha & \alpha\beta & \beta\alpha & \beta\beta \end{matrix} \\ \begin{pmatrix} \sigma_{\alpha\alpha\alpha\alpha} & \sigma_{\alpha\alpha\alpha\beta} & \sigma_{\alpha\alpha\beta\alpha} & \sigma_{\alpha\alpha\beta\beta} \\ \sigma_{\alpha\beta\alpha\alpha} & \sigma_{\alpha\beta\alpha\beta} & \sigma_{\alpha\beta\beta\alpha} & \sigma_{\alpha\beta\beta\beta} \\ \sigma_{\beta\alpha\alpha\alpha} & \sigma_{\beta\alpha\alpha\beta} & \sigma_{\beta\alpha\beta\alpha} & \sigma_{\beta\alpha\beta\beta} \\ \sigma_{\beta\beta\alpha\alpha} & \sigma_{\beta\beta\alpha\beta} & \sigma_{\beta\beta\beta\alpha} & \sigma_{\beta\beta\beta\beta} \end{pmatrix} \end{array}\right]$$

$$= \begin{array}{c} \begin{matrix} \alpha & \beta \end{matrix} \\ \begin{pmatrix} \sigma_{\alpha\alpha\alpha\alpha} + \sigma_{\alpha\beta\alpha\beta} & \sigma_{\alpha\alpha\beta\alpha} + \sigma_{\alpha\beta\beta\beta} \\ \sigma_{\beta\alpha\alpha\alpha} + \sigma_{\beta\beta\alpha\beta} & \sigma_{\beta\alpha\beta\alpha} + \sigma_{\beta\beta\beta\beta} \end{pmatrix} \end{array} . \qquad (5)$$

Hence, 2D FID of the DQ radical is expressed as

$$s(t_1, t_2) = \mathrm{Tr}[(S_x + \mathrm{i}\, S_y)\sigma_{DQ}(t_1, t_2)] = \sigma_{\beta\alpha\alpha\alpha}(t_1, t_2) + \sigma_{\beta\beta\alpha\beta}(t_1, t_2) \ . \qquad (6)$$

2.2. ESE J Spectroscopy

The ESE J method is performed by the pulse sequence shown in Fig. 1b. FID signals on ESE which is obtained by $\pi/4$ and π pulses are recorded as a function of pulse interval t_1 and the FID signals are Fourier transformed to give ESE⊗FT-EPR spectra as a function of t_1 or they are Fourier transformed as with the both t_1 and t_2 domains to give 2D expression. This method is based on the fact that the ESE-FT-EPR spectrum of SCRP obtained by Fourier transformation for the time domain of t_2 changes its spectral pattern with the pulse interval t_1, as is shown in the following.

As in Eq. (1), time evolution of the density operator under the pulse sequence of Fig. 1b is expressed as

$$\sigma(t_1,t_2) = \exp(-\mathrm{i}\mathscr{H}_0 t_2)\exp(-\mathrm{i}\mathscr{H}_0 t_1)R_\pi^{-1}\exp(-\mathrm{i}\mathscr{H}_0 t_1)R_{\pi/4}^{-1}\sigma(0) \times R_{\pi/4}\exp(\mathrm{i}\mathscr{H}_0 t_1)R_\pi\exp(\mathrm{i}\mathscr{H}_0 t_1)\exp(\mathrm{i}\mathscr{H}_0 t_2)\ , \tag{7}$$

where R_π and $R_{\pi/4}$ are rotation matrices for the π and $\pi/4$ MW pulses. We assume here also that J is kept constant during the data sampling period. By using the following initial density matrix $\sigma(0)$ for the triplet precursor, Eq. (9) can be derived from Eq. (7):

$$\sigma(0) = \begin{array}{c} \begin{matrix} \alpha\alpha & \alpha\beta & \beta\alpha & \beta\beta \end{matrix} \\ \begin{pmatrix} 1/3 & & & \\ & 1/6 & & \\ & & 1/6 & \\ & & & 1/3 \end{pmatrix} \end{array}, \tag{8}$$

$\sigma(t_1,t_2) =$

$$= \begin{pmatrix} 3+\frac{1}{2} & \frac{1}{2}(\mathrm{e}^{-\mathrm{i}4\pi Jt_1} \times \mathrm{e}^{\mathrm{i}(\Omega_\mathrm{b}-2\pi J)t_2}) & \frac{1}{2}(\mathrm{e}^{-\mathrm{i}4\pi Jt_1} \times \mathrm{e}^{\mathrm{i}(\Omega_\mathrm{a}-2\pi J)t_2}) & \frac{1}{2}(\mathrm{e}^{2\mathrm{i}(\Omega_\mathrm{a}-\Omega_\mathrm{b})t_2}) \\ \frac{1}{2}(\mathrm{e}^{\mathrm{i}4\pi Jt_1} \times \mathrm{e}^{-\mathrm{i}(\Omega_\mathrm{b}-2\pi J)t_2}) & 3-\frac{1}{2} & \frac{1}{2}(\mathrm{e}^{\mathrm{i}(\Omega_\mathrm{a}-\Omega_\mathrm{b})t_2}) & -\frac{1}{2}(\mathrm{e}^{\mathrm{i}4\pi Jt_1} \times \mathrm{e}^{\mathrm{i}(\Omega_\mathrm{a}+2\pi J)t_2}) \\ \frac{1}{2}(\mathrm{e}^{\mathrm{i}4\pi Jt_1} \times \mathrm{e}^{-\mathrm{i}(\Omega_\mathrm{a}-2\pi J)t_2}) & \frac{1}{2}(\mathrm{e}^{-\mathrm{i}(\Omega_\mathrm{a}-\Omega_\mathrm{b})t_2}) & 3-\frac{1}{2} & -\frac{1}{2}(\mathrm{e}^{\mathrm{i}4\pi Jt_1} \times \mathrm{e}^{\mathrm{i}(\Omega_\mathrm{b}+2\pi J)t_2}) \\ \frac{1}{2}(\mathrm{e}^{-2\mathrm{i}(\Omega_\mathrm{a}+\Omega_\mathrm{b})t_2}) & -\frac{1}{2}(\mathrm{e}^{-\mathrm{i}(\Omega_\mathrm{a}+2\pi J)t_2}) & -\frac{1}{2}(\mathrm{e}^{-\mathrm{i}4\pi Jt_1} \times \mathrm{e}^{-\mathrm{i}(\Omega_\mathrm{b}+2\pi J)t_2}) & 3+\frac{1}{2} \end{pmatrix}. \tag{9}$$

Equation (9) indicates that one quantum coherence of SCRP changes its phase by the MW pulses, and it is given as a function of $4\pi Jt_1$.

Using Eq. (9), the FID signals are given by

$$\begin{aligned} s(t_1,t_2) &= \mathrm{Tr}[S_+\sigma(2t_1,t_2)] \\ &= \frac{1}{2}\exp(-\mathrm{i}4\pi Jt_1)\left[\exp\left(\mathrm{i}(\Omega_\mathrm{b}-2\pi J)t_2\right)+\exp\left(\mathrm{i}(\Omega_\mathrm{a}-2\pi J)t_2\right)\right] \\ &\quad -\frac{1}{2}\exp(\mathrm{i}4\pi Jt_1)\left[\exp\left(\mathrm{i}(\Omega_\mathrm{a}+2\pi J)t_2\right)+\exp\left(\mathrm{i}(\Omega_\mathrm{b}+2\pi J)t_2\right)\right]. \end{aligned} \tag{10}$$

Fourier transformation of $s(t_1, t_2)$ in the time domain of t_2 gives a FT-EPR spectrum for a given pulse interval t_1, and its real part is expressed as

$$
\begin{aligned}
s(t_1, \Omega_2) = & -\frac{1}{2}\cos(4\pi J t_1)\frac{\Gamma}{[\Omega - (\Omega_b - 2\pi J)]^2 + \Gamma^2} \\
& + \frac{1}{2}\sin(4\pi J t_1)\frac{\Omega - (\Omega_b - 2\pi J)}{[\Omega - (\Omega_b - 2\pi J)]^2 + \Gamma^2} \\
& - \frac{1}{2}\cos(4\pi J t_1)\frac{\Gamma}{[\Omega - (\Omega_a - 2\pi J)]^2 + \Gamma^2} \\
& + \frac{1}{2}\sin(4\pi J t_1)\frac{\Omega - (\Omega_a - 2\pi J)}{[\Omega - (\Omega_a - 2\pi J)]^2 + \Gamma^2} \\
& + \frac{1}{2}\cos(4\pi J t_1)\frac{\Gamma}{[\Omega - (\Omega_a + 2\pi J)]^2 + \Gamma^2} \\
& + \frac{1}{2}\sin(4\pi J t_1)\frac{\Omega - (\Omega_a + 2\pi J)}{[\Omega - (\Omega_a + 2\pi J)]^2 + \Gamma^2} \\
& + \frac{1}{2}\cos(4\pi J t_1)\frac{\Gamma}{[\Omega - (\Omega_b + 2\pi J)]^2 + \Gamma^2} \\
& + \frac{1}{2}\sin(4\pi J t_1)\frac{\Omega - (\Omega_b + 2\pi J)}{[\Omega - (\Omega_b + 2\pi J)]^2 + \Gamma^2} \quad , \qquad (11)
\end{aligned}
$$

where Γ is a line width parameter.

Equation (11) indicates that a dispersion component appears in the spectrum, and the spectral pattern changes its phase with t_1 by a cycle of $1/2J$. By performing Fourier transformation of Eq. (11) also for the time domain of t_1, 2D expression giving cross spots having a separation of $2J$ along each frequency axis can be obtained as is shown later. This method may be useful for obtaining information about the spin-spin interaction in SCRPs and to evaluate the coupling value J. One problem in this method is that the SCRPs should have a T_2^* value long enough for recording a series of ESE signals.

3. Experimental Procedure

3.1. Materials

ZnTPPS was prepared from H_2TPPS and zinc acetate hydrate supplied from Strum and Wako chemicals, respectively. Prepared ZnTPPS was purified by the

procedure in the literature [11]. DQ and CTAC used were commercial ones (Wako chemicals). The micellar solution with a micelle concentration of about 1 mM was prepared by taking into account the fact that an aggregation number and a critical micelle concentration are 105 and 1.4 mM in water, respectively [11]. The solution was thoroughly deaerated with several freeze-pump-thaw cycles on a high vacuum line, and sealed in a Pyrex tube.

3.2. EPR Measurements

EPR measurements were performed with a Bruker ESP-380E spectrometer with a dielectric resonator. The measurements were carried out at 25°C. The sample temperature was controlled by a Bruker B-VT2000. In EPR measurements, MW pulses were synchronized to the laser pulses. Photoirradiation to the micellar solution of ZnTPPS and DQ was made with the second harmonics (532 nm) of a Spectra Physics Quanta-Ray GCR-14SNd:YAG laser with a repetition rate of 10 Hz.

In the one-dimensional FT-EPR experiments, duration and field strength of the MW pulse were about 10 ns and 0.6 mT, respectively. The quadrature FIDs were recorded in a step of 10 ns by 512 steps with CYCLOPS phase cycling. The missing part of FIDs during the instrumental dead time of about 88 ns was extrapolated with the LPQRD method [14]. The phase of FT-EPR spectra showing CIDEP effects was corrected by the spectra under a thermal spin equilibrium.

In 2D nutation experiments, two cases with different time delays of 1 and 10 μs from the laser excitation were examined. The duration of the 1 kW MW pulse is incremented in steps of 10 ns by 128 steps with the CYCLOPS phase cycling routine. Without extrapolation of lost parts of FID during the instrumental dead time, complex 2D FID matrices of 64×128 were apodized with the Hanning window in each dimension and zero-filled to 256×512 before the 2D complex FT.

In the ESE J spectroscopy, FT-EPR spectra were obtained by Fourier transformation of FID on the ESE obtained by $\pi/4$ and π pulses at the delay time of 900 ns from the laser excitation. These ESE-FT-EPR spectra were measured in a series of pulse intervals incremented in steps of 10 ns.

4. Experimental Results and Discussion

4.1. 2D FT-EPR Nutation Spectroscopy

Details of analyses of the 1D FT-EPR spectra for the photoinduced electron transfer reaction of ZnTPPS and DQ in a micellar solution are presented elsewhere [11, 15]. It is noted, however, that 1D FT-EPR spectra recorded before nearly 7 μs after photoirradiation can be assigned mostly to those of the SCRP. After 7 μs, the EPR spectra can be assigned as arising mainly from the DQ radical in the dissociated state. The oxidized ZnTPPS radical is not observed in

ordinary FT-EPR spectra, because of its broad linewidths due to the unresolved hyperfine couplings; its FID decays before data sampling [16].

The 2D nutation spectra recorded for $\tau_d = 1$ and 10 μs are shown in Fig. 2. These 2D nutation spectra with these different delay times indicate explicitly different correlations in each peak between EPR and nutation frequencies, reflecting overwhelming presence of the SCRP at $\tau_d = 1$ μs in solution. It is seen from the spectra that the nutation frequencies and the signal intensities are not symmetric as with the on-resonance position. These can be attributable to the off-resonance effects discussed in the previous paper [12]. It must be noted that the signals observed in the 2D nutation spectra of the present system are much broader than those reported previously for the photochemical hydrogen abstraction reaction of acetone-d_6 from 2-propanol-d_8 [12]. This large broadening in the present system may be attributed to inhomogeneous line broadening by the presence of many sets of nuclear spin configurations in the partner ZnTPPS radical.

The computer simulation of the 2D nutation EPR spectra were performed by assigning a triplet state as a precursor. As mentioned above, the effects of contribution of the ZnTPPS radical to the nutation spectra of the SCRP were taken by tracing the spin density operator over the subspace of the ZnTPPS radical. The EPR spectrum of the ZnTPPS radical was approximated by a Gaussian type with a full width of half maximum of 16.5 MHz and 11 lines with separation of 4.0 MHz. The other parameters used for the simulation calculation were 4.99 MHz (DQ) and −5.60 MHz (Zn-TPPS) for center of the spectrum of

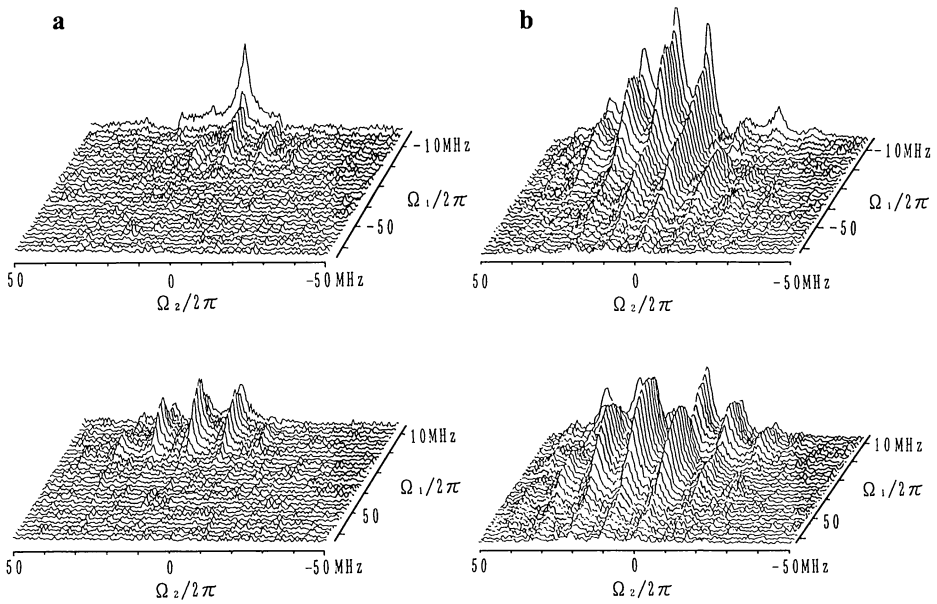

Fig. 2. 2D FT-EPR nutation spectra of ZnTPPS/DQ/CTAC micellar solution at the delay times τ_d of **a** 1 μs and **b** 10 μs. The ω_1 and ω_2 are the nutation and the EPR frequencies, respectively.

each partner, 2.0049 (DQ) and 2.0025 (ZnTPPS) for the g values, 5.40 MHz for the hyperfine coupling of DQ, and $B_1 = 0.421$ mT. The J value was treated as a variable.

The 2D nutation spectra obtained by the calculation for different J values are shown in Fig. 3. Fig. 4 is the nutation spectra at some specific EPR frequencies which are obtained by slicing the 2D spectra at the given frequencies. The calculated spectra are not necessarily so sensitive to J, especially in the cases with small J. However, one can see that the calculated spectra reproduce well the experimental spectra. We estimated that $|J|$ may be smaller than 0.3 MHz from comparison with the calculated spectra.

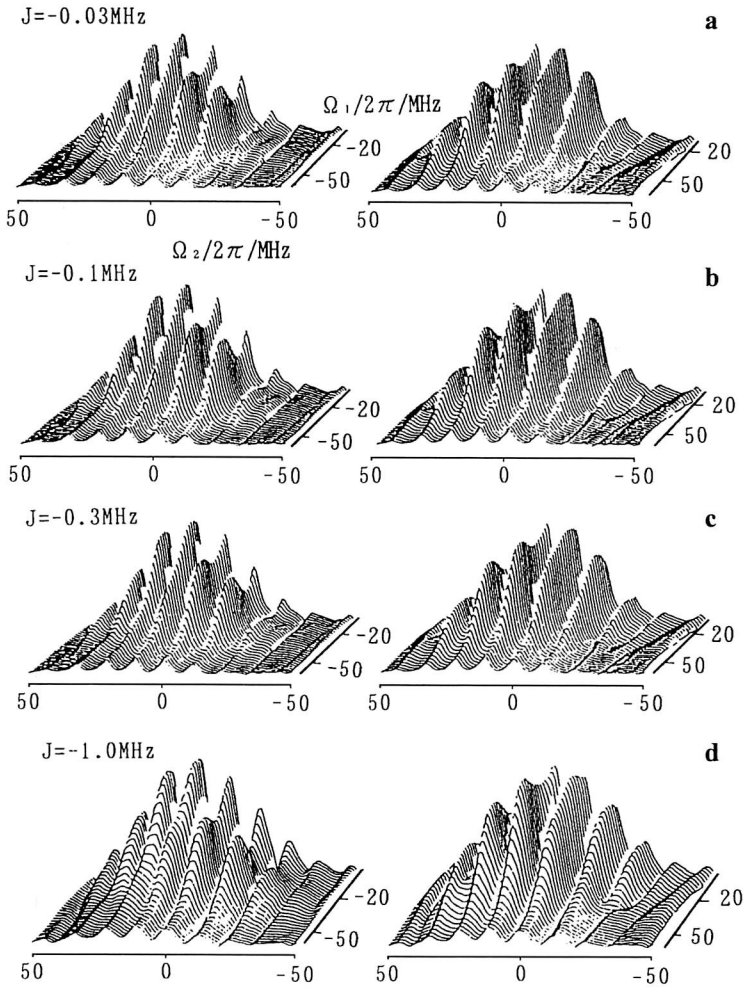

Fig. 3. Calculated nutation spectra with four different J values: -0.03 MHz (**a**), -0.1 MHz (**b**), -0.3 MHz (**c**), and -1.0 MHz (**d**). The parameters used are shown in text.

4.2. ESE J Spectroscopy

4.2.1. Model Calculations

2D J spectroscopy in NMR is an useful technique to extract spin-spin couplings from complex spectral systems [7]. SCRPs seem to be new challenging subjects for this method. In case of SCRPs, however, the interacting spins are not in a thermal equilibrium and the J values would vary dynamically accompanied by

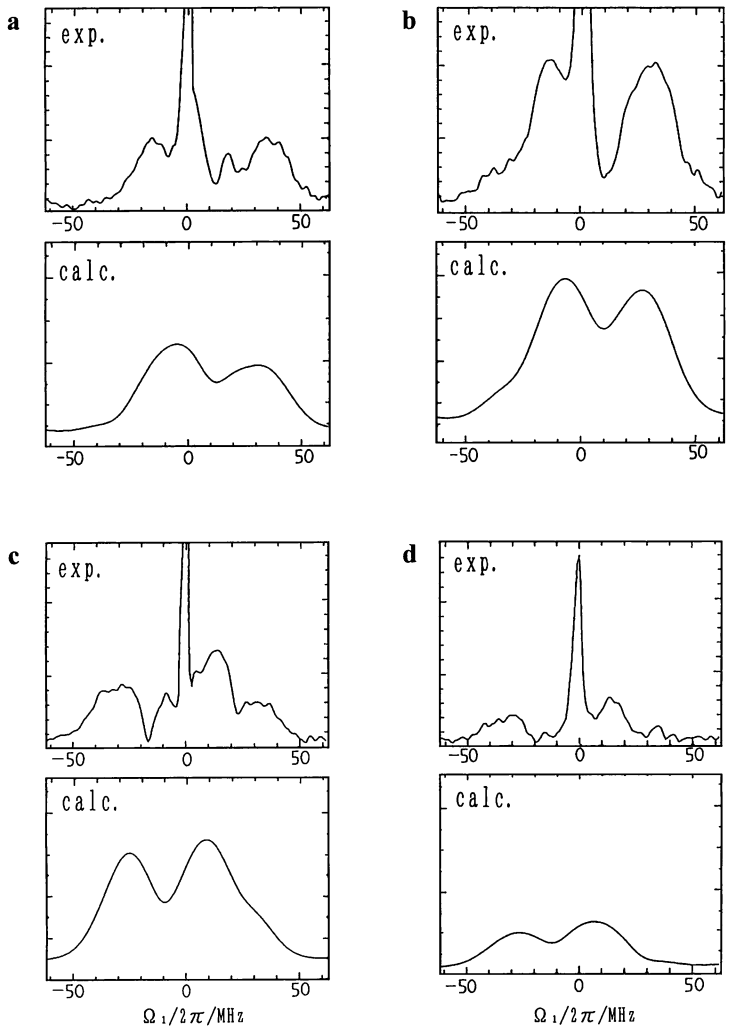

Fig. 4. Nutation Spectra at EPR frequencies ($\Omega_2/2\pi$) of **a** 15.625 MHz, **b** 10.547 MHz, **c** −5.859 MHz, and **d** −11.328 MHz. The peaks at zero frequency in the experimental spectra are architecture from the instrument.

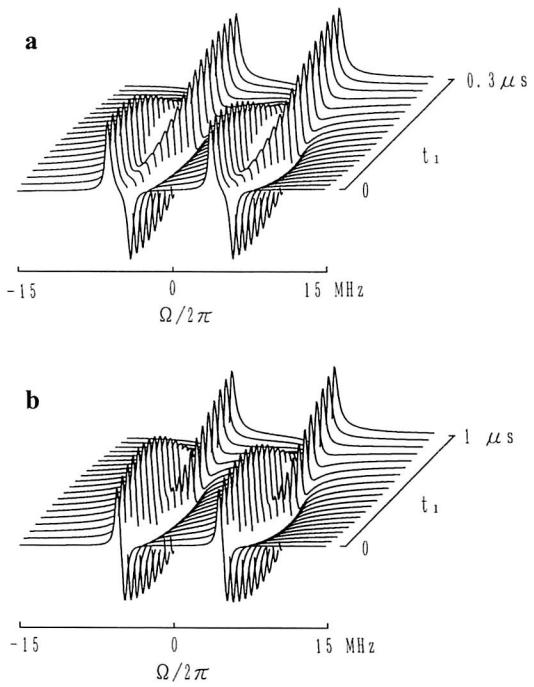

Fig. 5. ESE-FT-EPR spectra calculated as a function of pulse interval t_1: $J = -1$ MHz (**a**) and $J = -0.3$ MHz (**b**). The other parameters used are: $\Omega_a/2\pi = -5$ MHz, $\Omega_b/2\pi = 5$ MHz, $\Gamma/2\pi = 0.3$ MHz.

mutual motion of the radicals in solvent cages. In advance of experimental analyses, we attempted model calculations for application of this method to

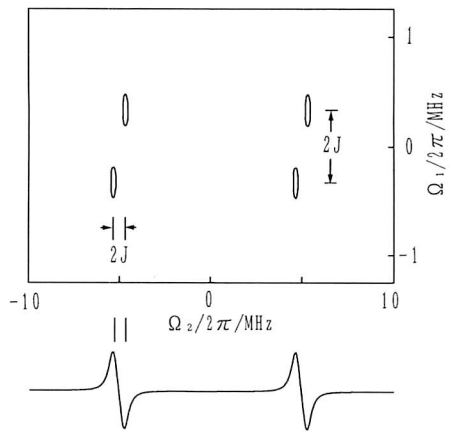

Fig. 6. 2D contour plot of ESE J method. $\Omega_{2a}/2\pi = -5$ MHz, $\Omega_{2b}/2\pi = 5$ MHz, $J = -0.3$ MHz, and $\Gamma_1/2\pi = \Gamma_2/2\pi = 0.3$ MHz.

SCRPs. The J value is assumed to be constant during the data sampling in this case, too for simplicity. The precursor is taken to be a triplet state as before.

Figure 5 shows a series of ESE-FT-EPR spectra calculated as a function of pulse interval t_1 for the cases of $J = -1.0$ and -0.3 MHz, respectively. The

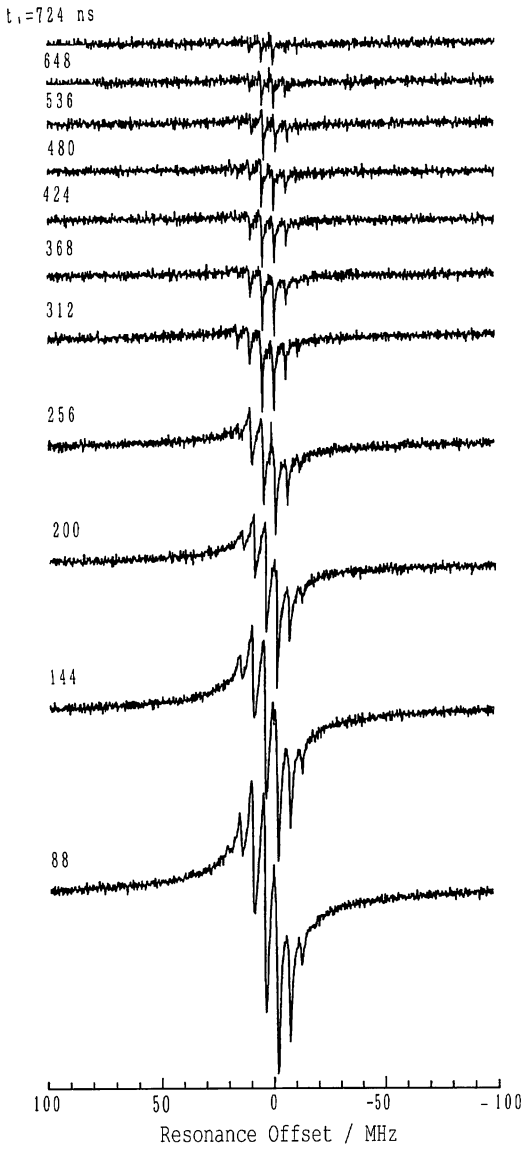

Fig. 7. ESE-FT-EPR spectra observed for the ZnTPPS/DQ/CTAC solution at 25°C and at delay time τ_d of 900 ns as a function of pulse intervals t_1.

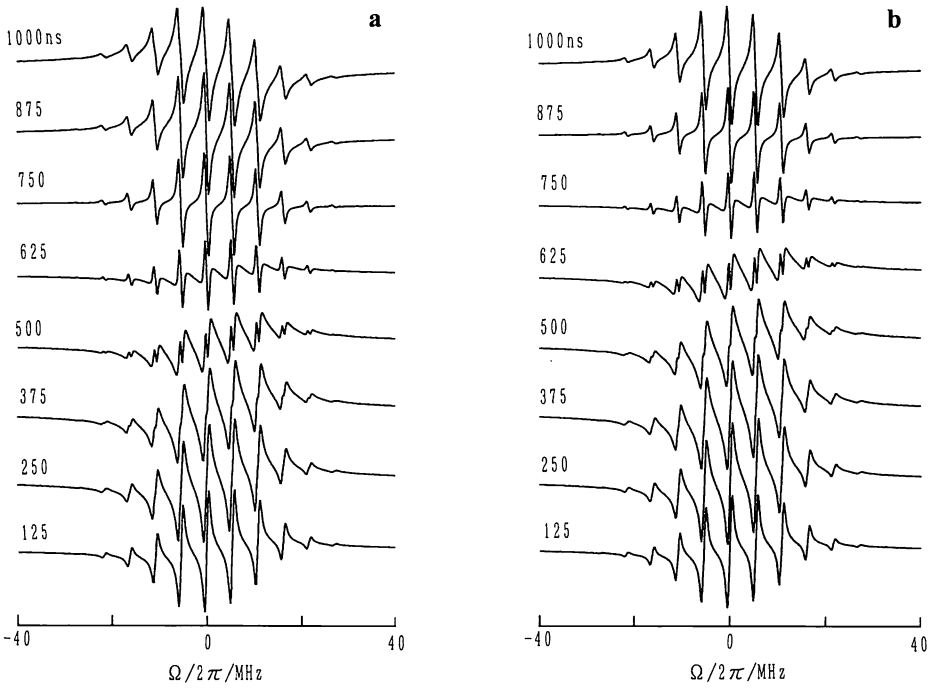

Fig. 8. ESE-FT-EPR spectra of SCRP calculated for different t_1 and for $J = -0.35$ MHz (**a**) and $J = -0.3$ MHz (**b**).

parameters used are shown in the figure caption. A decrease of the signal intensities by the spin relaxation with increasing pulse intervals is not taken into account in the calculation. Fig. 5 clearly indicates that the A/E antiphase pattern of the SCRP changes its phase with the pulse interval by a function of $4\pi J t_1$, and such changes must be a sensitive probe for J. Fig. 6 is 2D plots obtained by Fourier transformation of magnetization in both t_1 and t_2 time domains. The peak separations indicated by arrows in the figure correspond to the $2J$ value.

4.2.2. ESE-FT-EPR Spectra of ZnTPPS/DQ/CTAC Reaction System

Figure 7 shows the spectral changes with pulse interval t_1 observed for the ZnTPPS/DQ/CTAC reaction system at the delay time τ_d of 900 ns from the laser pulse. For this delay time the EPR signals mostly come from the SCRP. Fig. 8 shows calculated spectra for the DQ radical in the SCPR for different pulse intervals, where signals from the partner ZnTPPS radical are omitted, though the experimental data contain the broad signals from the ZnTPPS radical. Unfortunately the ESE-FT-EPR spectrum appreciably decays at longer t_1 than 600 ns. However one can not see clear phase inversion of the A/E antiphase

pattern before $t_1 = 600$ ns. Though comparison over the wide range of pulse intervals is difficult, one can estimate that $|J|$ would be at least smaller than 0.35 MHz. It should be noted that the spectra taken at the large t_1 might contain contribution from the DQ radical in the dissociated state.

5. Conclusive Remarks

We applied the two 2D FT-EPR methods to examination of the SCRP formed in the photoinduced electron transfer reaction in the ZnTPPS/DQ/CTAC micellar solution system. By the 2D FT-EPR nutation method, we estimated the absolute value of J to be smaller than 0.3 MHz. One advantage of this method is to enable one to observe SCRP signals partly separated from those of radicals existing as free ions.

We also presented that the second new method, ESE J spectroscopy, is a useful technique for investigation of SCRPs. However, there may be cases where detailed analyses of SCRPs are difficult due to short spin relaxation times of SCRPs. For the present case, we estimated the upper limit of the absolute value of J to be 0.35 MHz, which is consistent with the data from the nutation method. Dynamic behavior of spin-spin interaction in SCRPs is an interesting problem in the field of spin chemistry. Further analyses by these methods by taking into account the effects of dynamic changes of J are in progress.

Acknowledgements

This work was financially supported by Grants-in-Aid of Scientific Researches No. 06640711(MI), No. 04242102(SY), and No. 6239208(SY) from the Ministry of Education, Science and Culture of Japan. The authors are grateful to Prof. Shozo Tero-Kubota and Dr. Kimio Akiyama of our institute for their help in the FT-EPR measurements.

References

[1] Steiner R., Utrich T.: Chem. Rev. **89**, 51 (1989)
[2] Kevan L., Bowman M.K. (eds.): Modern Pulsed and Continuous Wave Electron Spin Resonance. New York: Wiley 1990.
[3] Thurnauer M.C., Bowman M.K., Norris J.R.: FEBS Lett. **100**, 309 (1979)
[4] Thurnauer M.C., Norris J.R.: Chem. Phys. Lett. **76**, 557 (1980)
[5] Thurnauer M.C., Rutherfold A.W., Norris J.R.: Biochem. Biophys. Acta **682**, 332 (1982)
[6] Buckley C.D., Hunter D.A., Hore P.J., McLauchlan K.A.: Chem. Phys. Lett. **135**, 307 (1987)
[7] Ernst R.R., Bodenhauser G., Woukaun A. (eds.): Principles of Nuclear Magnetic Resonance in One and Two dimensions. New York: Oxford 1987.
[8] Harashanori K., Levanon H., Tang T., Bowman M.K., Norris M.K., Gust D., Moore T.A., Moore A.L.: J. Am. Chem. Soc. **112**, 6477 (1990)
[9] Kroll G., Pluschau M., Dinse K.-P., van Willigen H.: J. Chem. Phys. **93**, 8709 (1990)

[10] Schublin S., Hohner A., Ernst R.R.: J. Magn. Reson. **13**, 196 (1974)
[11] Levestein R.R., van Willigen H.: Chem. Phys. Lett. **187**, 415 (1991)
[12] Hanaishi R., Ohba Y., Akiyama K., Yamauchi S., Iwaizumi M.: J. Magn. Reson. (in press); Hanaishi R., Ohba Y., Akiyama K., Iwaizumi M.: J. Chem. Phys. **103**, 4819 (1995)
[13] Fano U.: Rev. Modern Phys. **29**, 74 (1957)
[14] Tang J., Lin C.P., Norris J.R.: J. Magn. Reson. **62**, 167 (1985)
[15] Hanaishi R., Ohba Y., Yamauchi S., Iwaizumi M.: J. Phys. Chem. (submitted)

Author's address: Prof. Dr. Masamoto Iwaizumi, Institute for Chemical Reaction Science, Tohoku University, Katahira 2-1-1, Aoba-ku, Sendai 980, Japan